Aust. Met. Mag. 36 (1988) 11-16

On the horizontal resolution of fronts in numerical weather prediction models

Michael J. Reeder* and Roger K. Smith†

(Manuscript received January 1988; revised March 1988)

The ability of current numerical weather prediction models to capture frontogenesis and to determine frontal motion is explored using a two-dimensional numerical model. The model was developed recently by the authors specifically to study the dynamics of the Australian summertime 'cool change', but it is not restricted to such fronts. Attention is focused here on the ability of a simulation with a very coarse grid (150 km horizontal resolution) to represent the dynamics of a frontogenetically-active model cold front in a simulation with a relatively fine grid (15 km horizontal resolution). Two intermediate resolution simulations are discussed also, one with a horizontal grid spacing of 50 km, the other with 100 km spacing.

We conclude that a resolution between 50 km and 100 km is adequate for capturing frontal scale motions and for predicting frontal movement whereas a model with a 150 km horizontal grid is generally inadequate.

Our calculations show also that the surface location of the maximum relative vorticity component in the vertical provides a more robust indicator of frontal position than that of the maximum horizontal temperature gradient; it is less dependent on the horizontal resolution and less sensitive to the presence of geographically-fixed frontogenesis such as differential heating across a coastline.

Introduction

Much of the significant weather of southern Australia is associated with the passage of cold fronts and the prediction of these poses an important forecasting problem. The prediction difficulty increases during the late spring and summer when there is a large thermal contrast between continental and maritime air masses in the region. At these times of the year, incorrect forecasts of the arrival time of a front may lead to substantial (10–15 K) errors in maximum temperature forecasts at a given location.

In a recent paper, Wilson et al. (1987) have sought to establish forecast verification procedures for line-type phenomena using cold fronts in southeastern Australia as the principal application. They showed, *inter alia*, that on average the movement of such fronts is underestimated in prognoses. Since a major source of forecast guidance in the region is provided by numerical prognoses using the Australian Regional Primitive Equation (ARPE) model (Leslie et al. 1985), the question arises as to what extent the resolution provided by the model (currently 150 km in the horizontal and 12 levels in the vertical) is adequate for forecasting frontal movement and development. In this paper we seek to address this resolution question more widely using a two-dimensional numerical model that we developed specifically to study the dynamics of summertime cold fronts (or 'cool-changes') that occur in southeastern Australia (Reeder and Smith 1986, 1987; Reeder 1986).

The model

The model is anelastic and hydrostatic with a stretched vertical grid and uses the stream-function-vorticity form of the equations as the basis for numerical solution. The computational domain is 15 km high and 4500 km long and has open boundaries at both ends. Initial conditions are prescribed in the form of wind and temperature fields representing idealised vertical cross-sections through a typical pre-existing disturbance, prior to its amplification to an intense front-trough system. In essence, these cross-sections correspond with a warm pre-frontal

*Laboratory for Atmospheres, NASA Goddard Space Flight Center, USA.

†DFVLR Institute for Atmospheric Physics, West Germany. (Permanent affiliation: Meteorologisches Institut Universität München, Theresien str. 37, 8000 München 2, West Germany.)

northerly airstream embedded in a zonal shear flow in thermal wind balance with a meridional temperature gradient. An initial ageostrophic vertical circulation is imposed also, being that required to ensure that the frontal development continues in a quasi-balanced state. Further details of the model and the initialisation procedure are given by Reeder and Smith (1987) and the initial fields are shown in Figs 4(a), 5(a) and 6(a) in that paper.

The results to be presented below are based primarily on four 24-hour model integrations with different grid resolutions: a fine resolution simulation with a horizontal grid spacing Δx of 15 km and 51 vertical levels, corresponding with a *mean** vertical grid spacing $\overline{\Delta z}$ of 300 m; two coarser resolution simulations, one with Δx = 100 km and 21 levels ($\overline{\Delta z}$ = 750 m), the other with Δx = 150 km and 16 levels; and an intermediate resolution simulation with Δx = 50 km and 26 levels ($\overline{\Delta z}$ = 600 m). We shall regard the fine resolution calculation as the control simulation. The coarser resolution integrations are broadly typical of current numerical weather prediction models including the ARPE model in particular, while the intermediate resolution simulation is typical of some fine-mesh mesoscale models now in use. The number of levels chosen for each integration roughly represents the finest vertical resolution reported in published modelling studies of comparable horizontal resolution.

Four analogous calculations in which the front approaches a heated land mass will be referred to also. These are based on an extended version of the model described by Reeder (1986). In these, the initial position of the surface front is 360 km offshore and heating of the land mass commences after 6 hours of integration when, in the fine resolution simulation, the front is 224 km offshore. Differential heating continues for a further 12 hours, after which no further heat is added.

The horizontal diffusivity in the fine resolution simulation is 3 x 10^4 m^2 s^{-1}, while in the intermediate, coarse and very coarse simulations it is increased by the factors $(50/15)^2$, $(100/15)^2$ and $(150/15)^2$, respectively, to take account of the reduced horizontal resolution. In each integration vertical diffusion is neglected for simplicity.

Results

Figure 1 shows vertical cross-sections of the isotachs of along-front wind component v, and

*On account of the vertically-stretched grid, the actual grid spacing in the fine resolution calculation varies from 120 m near the surface to 0.8 km at 15 km. The model grid is stretched in a similar manner in the intermediate, coarse and very coarse simulations, wherein the grid spacing varies between 258 m and 1.84 km, 337 m and 2.2 km, and 500 m and 2.7 km, respectively.

Fig. 1 **(a) Isotachs of along-front velocity v and (b) streamlines of the ageostrophic cross-front circulation ψ_{ag}, each superimposed on the isentropes θ, for the fine mesh calculation (Δx = 15 km) at t = 18 hours. The corresponding isopleths for the very coarse mesh calculation (Δx = 150 km) are shown in (c) and (d), respectively. Contour intervals are: 5 m s^{-1} for v, 3 x 10^3 kg m s^{-1} for ψ_{ag}, and 5 K for θ.**

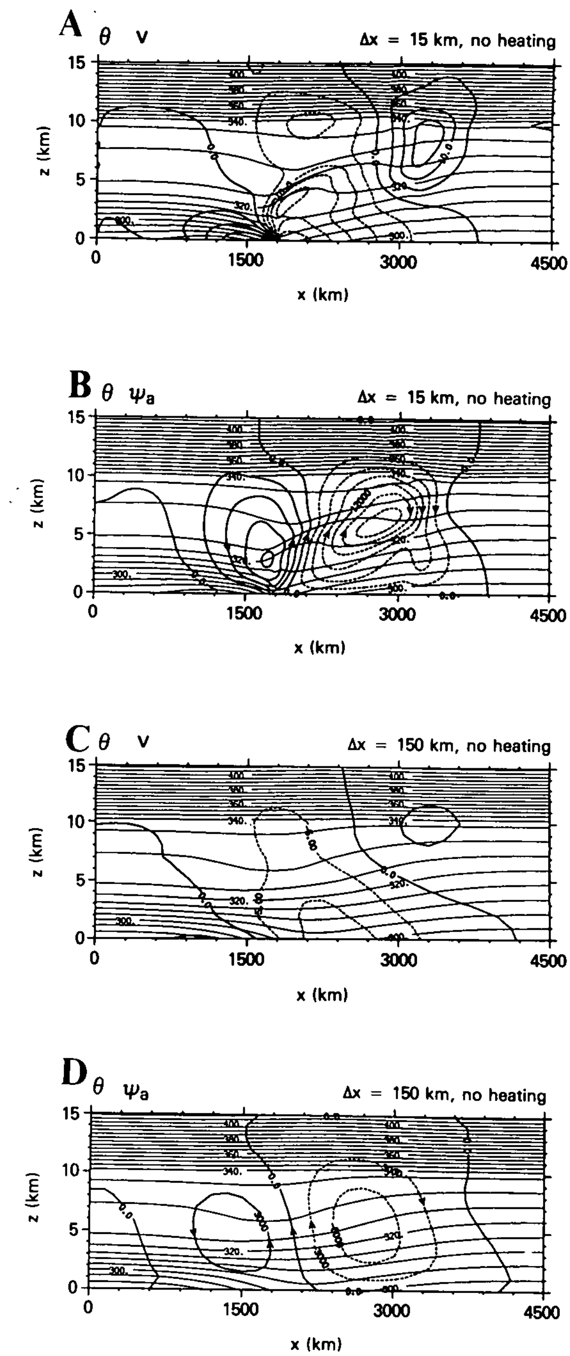

the streamlines of the ageostrophic cross-front circulation ψ_{ag}, each superimposed on the isentropes θ, for the fine mesh (Δx = 15 km) and very coarse mesh (Δx = 150 km) simulations, without diurnal heating, after 18 hours of integration. Comparison shows that whereas the very coarse mesh calculation captures the overall scale and sense of the cross-front circulation it fails to adequately represent much of the detail; in fact it predicts the cell in the warm air to slope in the wrong direction (cf. Figs 1(b) and 1(d)). Furthermore, the very coarse mesh calculation considerably underestimates the intensity of the circulation and hence its associated convergence. The effect of resolution on the ageostrophic circulation neatly exposes the dynamical effect it has on the surface frontogenesis processes. A reduction in surface convergence is accompanied, *inter alia*, by a reduction in the rate at which cyclonic vorticity is produced through the stretching of absolute vorticity, as well as a reduction in the rate at which the surface temperature gradient changes due to convergence itself. Moreover, a weaker ageostrophic circulation implies weaker Coriolis torques in the along-front direction and thereby a reduction in the acceleration of the along-front wind component (cf. Figs 1(a) and 1(c)). In turn, this is associated with a reduction in the along-front temperature advection by the pre and post-frontal low-level jets, and hence to a reduced rate of frontogenesis itself.

The effects of degraded resolution are so severe in the very coarse mesh integration that during the first 12 hours the strength of the surface front, as defined by the maximum surface (potential) temperature gradient $(\theta_x)_{max}$, weakens slightly before attaining a steady value of 1.5 K/km as evidenced by the time-series of $(\theta_x)_{max}$ shown in Fig. 2. In this case the frontolytic effects of horizontal diffusion exceed combined effects of the frontogenetic processes during the first half of the integration. In contrast, in the fine mesh calculation the surface front increases in strength by almost an order of magnitude during the first 12 hours, reaching a quasi-steady value of about 17 K/100 km. Shown also in Fig. 2 are times-series of $(\theta_x)_{max}$ for both the coarse (Δx = 100 km) and intermediate resolution (Δx = 50 km) runs. As in the fine mesh simulation, $(\theta_x)_{max}$ increases during the first 12 hours for these two calculations, thereafter maintaining nearly steady values of 3 K/km and 6 K/km respectively. The ratio of the steady-state values of $(\theta_x)_{max}$ of any two cases is roughly equal to the ratio of the respective values of Δx for the same two cases; therefore, the intensity of the simulated fronts are directly proportional to their horizontal resolution.

Using the nomenclature of Orlanski (1975), the associated frontal circulation is *meso-α* in scale

Fig. 2 Time-series of maximum surface potential temperature gradient $(\theta_x)_{max}$ for the four different resolution calculations: (a) without diabatic heating effects; and (b) with diabatic heating included. Units in K/100 km.

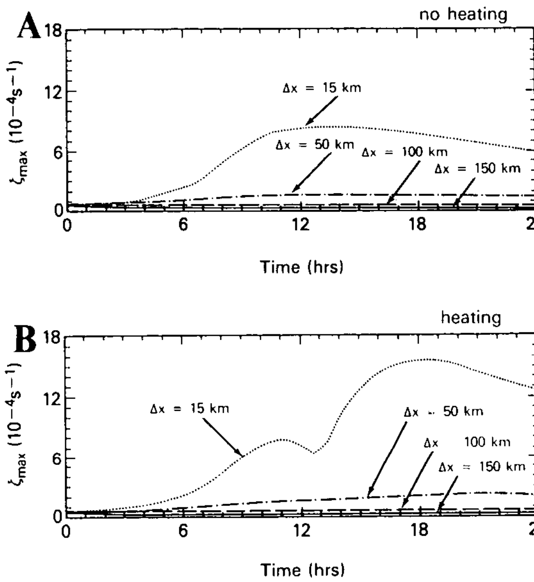

(200-2000 km), whereas the scale of the front itself is *meso-β* (20-200 km). The very coarse resolution calculation resolves the *meso-α* scale, albeit rather poorly, whereas the *meso-β* effects remain subgrid scale; consequently the very coarse resolution simulation fails to produce a surface front (see Fig. 2).

Similar results were obtained in a comparison of the fine, intermediate, coarse and very coarse mesh runs* when diurnal heating was included, but in this case the maximum surface gradient increased in all four simulations in response to the heating of the land; time-series of $(\theta_x)_{max}$ for these simulations are shown in Fig. 3.

The limitations of the very coarse mesh are even more severe when diurnal heating is present. Figure 3 shows the vertical velocity w, after 18 hours of integration, both with and without diurnal heating, for the fine mesh and very coarse mesh runs. In the fine mesh case the inclusion of diurnal heating leads to an intense updraft (~ 18 cm s^{-1}) in a narrow region in the vicinity of the surface front (cf. Figs 3(a) and 3(b)), the development of which has been discussed in detail by Reeder (1986) (see Fig. 6 of Reeder 1986 for details of the updraft structure). While this

*There is a small difference in the implementation of the diurnal heating in the fine mesh run. As outlined in Reeder (1986), the spatial gradient of sensible heat flux, representing the coastline, is spread over a distance 2Δx (i.e. 30 km). In the coarse and intermediate resolution calculations the heating gradient is confined to a distance Δx. Doubling the width of the transition zone in the fine mesh run *reduces* the relative impact of differential heating in this calculation.

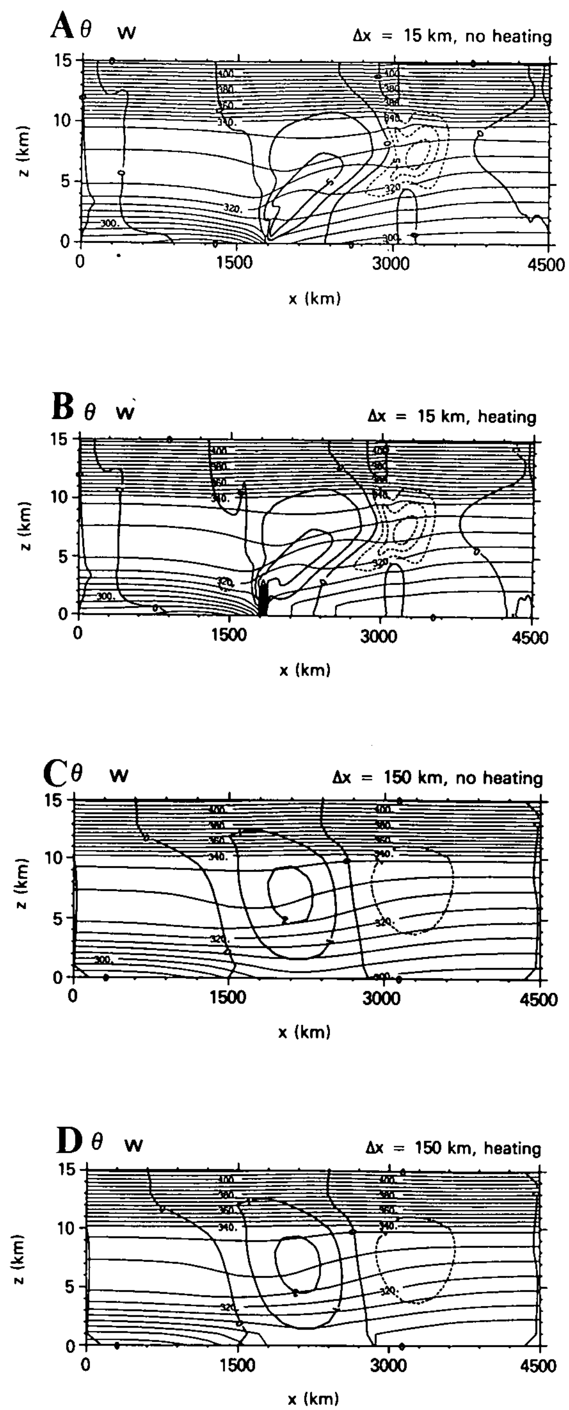

Fig. 3 **Isotachs of vertical velocity w superimposed on the isentropes θ at t = 18 hours for the fine resolution calculations: (a) without diurnal heating; and (b) with diurnal heating included. The corresponding isopleths for the very coarse resolution calculation are shown in (c) and (d), respectively. Contour intervals are: 2.5 cm s^{-1} for w in (a) and (b) and 1 cm s^{-1} in (c) and (d); and 5 K for θ.**

feature is highly localised it may play an important dynamical role, particularly in the initiation and organisation of pre-frontal convection (Reeder 1986). The pre-frontal updraft is below the resolution of the very coarse mesh model (cf. Figs 3(b) and 3(d)). In fact, the vertical velocity fields in the coarse mesh runs, with and without diurnal heating, are virtually identical (cf. Figs 3(c) and 3(d)). The same is true of the coarse mesh simulation (not shown). However, the intermediate mesh calculation (also not shown) exhibits a very weak intensification of the frontal circulation associated with diurnal heating, and appears to have about the maximum grid spacing capable of resolving this feature.

The effect of resolution on the frontal movement is of key interest to the forecaster. The effect is illustrated in Fig. 4 which shows time-series of x_θ, the position* of $(\theta_x)_{max}$ in the eight model simulations. Comparing first the runs without diurnal heating we note that resolution has a significant impact on the frontal position, and hence on the frontal speed. After 18 hours of integration the very coarse resolution forecast places the front nearly 290 km upstream of the fine resolution forecast, equivalent to a timing error of -7.4 hours, based on the mean translation speed of the front during the last 6 hours of the simulation. In contrast, the intermediate resolution simulation underestimates the front's progress by only 62 km (2 hours), while the coarse resolution calculation is in error by 172 km (4.7 hours). We note that the relative error in x_θ is approximately proportional to the grid spacing.

Figure 4 depicts also the analogous calculations with diurnal heating included. An outstanding feature of these time-series is a pronounced frontal acceleration as the front approaches the coastline, followed by a more gradual deceleration after crossing it, with the temporal scale of the acceleration and deceleration decreasing with increasing resolution. Differential diurnal heating acts to produce a local temperature gradient maximum at the coastline. The apparent frontal acceleration is due to the formation of a new 'front', as defined by $(\theta_x)_{max}$, at the coastline. This process has been discussed by Reeder (1986) and, more recently, by Physick (1988). The precise details of the apparent onshore acceleration depend intimately on the relative magnitudes of the coastal and frontal gradients; the initial distance of the front from the coast; and the horizontal resolution. Consider the coarse resolution calculation. As the front approaches the coastline, (non-linear) superposition of the frontal and coastal gradients produces a relative maximum in the gradient *between* the front and the

*The position of the surface maxima are calculated by fitting a cubic equation through the model grid-point data.

Fig. 4 Time-series of x_θ, the position of $(\theta_x)_{max}$, in the four different resolution calculations: (a) without diabatic heating; and (b) with diabatic heating included. Units in 10^2 km.

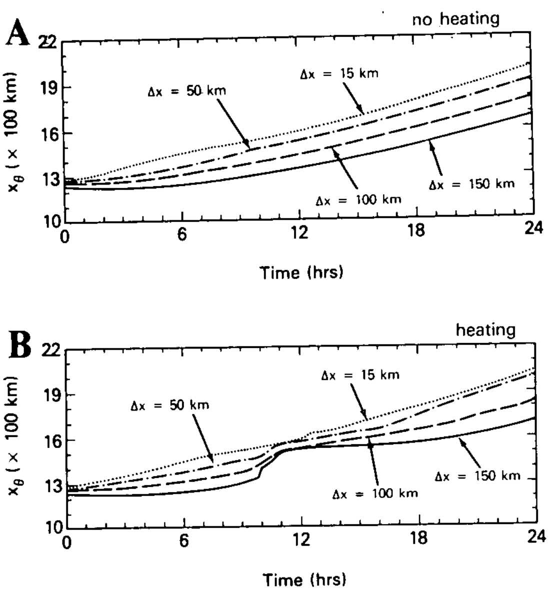

coast, which in turn is interpreted as a frontal acceleration*. Conversely, after the (original) front crosses the coastline, a similar superposition would lead to an apparent deceleration. As Δx is decreased, so too are the horizontal scales of the frontal and coastal gradients. Thus, the interaction of the frontal and coastal gradients occur over proportionately smaller time and space scales, which in turn explains why the apparent onshore surge occurs over progressively shorter time intervals as the model resolution decreases.

An alternative measure of the evolution of frontal strength is provided by time-series of $(\zeta)_{max}$, the maximum relative vorticity at the surface. For the simulations we have described, such time-series show a similar behaviour to those for $(\theta_x)_{max}$; compare Fig. 5 with Fig. 2. Likewise, x_ζ, the position of $(\zeta)_{max}$, provides an alternative definition for the location of the surface front. In the foregoing model simulations, x_ζ and x_θ move at comparable speeds, with x_ζ leading x_θ. The distance separating these maxima decreases with both increasing resolution and increasing frontal intensity. For the models discussed herein the distance separating x_ζ and x_θ is typically about $1-2\Delta x$. Time-series of x_ζ for each simulation are shown in Fig. 6. The most prominent feature is the relative robustness of x_ζ to changes in resolution. Moreover, x_ζ is quite insensitive to the addition of diurnal heating. Although the eight simulations exhibit substantial differences, rather

*In a calculation where the heating across the coastline was relatively intense, the front appeared to jump to the coastline.

Fig. 5 As in Fig. 2, except for the vertical component of relative vorticity, ζ_{max}. Units are $10^{-4}s^{-1}$.

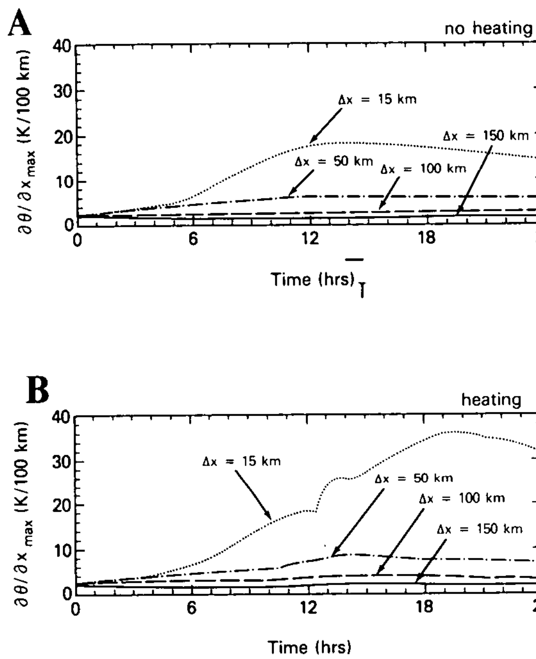

Fig. 6 As in Fig. 4, except for x_ζ, the position of ζ_{max}.

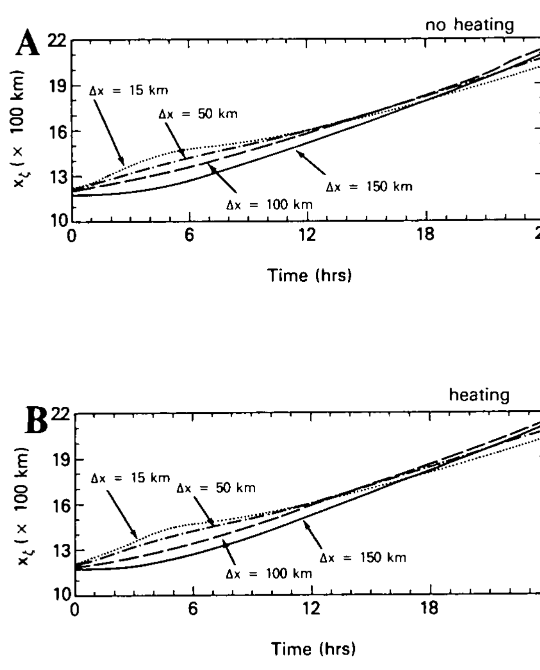

remarkably, after 18 hours, x_ζ are essentially identical in each forecast. At this time it is the coarse mesh forecast of x_ζ that shows least agreement with the fine mesh prediction. Nevertheless, the difference is only 27 km (0.7 hours) when diurnal heating is excluded and 61 km (1.7 hours) when it is included. These results suggest that the relative vorticity field, rather than the horizontal temperature gradient field, provides a more reliable and less ambiguous way of defining a front, a result that has been found also when applying the ARPE model to summertime cold fronts in southeastern Australia (K. McInnes, personal communication).

Conclusions

We have examined the limitations of horizontal resolution on the ability of numerical models to capture the dynamics of cold fronts. Our results suggest that current numerical weather prediction models with a horizontal grid typically of the order of 150 km are able to resolve the cross-frontal circulation, albeit poorly, but not the scale of the front, which is comparable with the grid spacing. Decreasing the horizontal grid size from 150 km to 50 km gives a significant improvement in the representation of a front and, in particular, in the determination of frontal speed. In contrast, a further threefold reduction in the grid size gives a relatively small additional improvement. We conclude that a horizontal grid size of between 50 km and 100 km is adequate for resolving frontal scale motions and for predicting frontal movement, which is in accord with the findings of Miyakoda and Rosati (1977).

We have shown that the speed of the surface front, as defined by $(\theta_x)_{max}$, decreases with decreasing horizontal resolution, the implication being that numerical weather prediction models using coarse horizontal grids may significantly underestimate the arrival time of the front. Our calculations show also that the location of $(\zeta)_{max}$ at the surface is a more robust indicator of frontal position than the location of $(\theta_x)_{max}$; in particular, it is less sensitive to the horizontal resolution and to the presence of differential heating across a coastline, itself a geographically-fixed frontogenetic effect.

References

Leslie, L.M., Mills, G.A., Logan, L.W., Gauntlett, D.J., Kelly, G.A., Manton, M.J., McGregor, J.L. and Sardie, J.M. 1985. A high-resolution primitive equation NWP model for operations and research. *Aust. Met. Mag.*, *33*, 11-35.

Miyakoda, K. and Rosati, A. 1977. One-way nested grid models: The interface condition and numerical accuracy. *Mon. Weath. Rev.*, *105*, 1092-107.

Orlanski, I. 1975. A rational subdivision of scales for atmospheric processes. *Bull. Am. met. Soc.*, *56*, 527-30.

Physick, W.L. 1988. Mesoscale modelling of a cold front and its interaction with a diurnally heated land mass. *J. Atmos. Sci.* (in press).

Reeder, M.J. 1986. The interaction of a cold front with a prefrontal thermodynamically well-mixed boundary layer. *Aust. Met. Mag.*, *34*, 137-48.

Reeder, M.J. and Smith, R.K. 1986. A comparison between frontogenesis in the two-dimensional Eady model of baroclinic instability and summertime cold fronts in the Australian region. *Q. Jl R. met. Soc.*, *112*, 293-313.

Reeder, M.J. and Smith, R.K. 1987. A study of frontal dynamics with application to the Australian summertime "cool change". *J. Atmos. Sci.*, *44*, 687-705.

Wilson, K.J., Barrell, S.L. and Del Beato, R. 1987. An approach to verifying prognoses of line phenomena and its application to fronts over southeastern Australia. *Mon. Weath. Rev.*, *115*, 1339-71.